
# Numerical Modeling of String/Barrier Collisions

S. Bilbao
University of Edinburgh, Room 1602, JCMB, Kings Buildings, Mayfield Rd., EH9 3JZ Edinburgh, UK
sbilbao@staffmail.ed.ac.uk

The collision of a string with a distributed rigid barrier plays a role in various musical instruments. The effects can range from minor but salient, as in the case of a freely vibrating guitar string in contact with the instrument neck, to major, as in the case of stringed instruments such as the sitar or tambura. Other examples are associated with playing gestures, such as the string/fretboard/finger interaction. Numerical design for such a highly nonlinear interaction, whether for purposes of model validation or sound synthesis, poses many challenges. The finite difference time domain method is applied here, in a Hamiltonian formulation, with collisions modelled through the use of a potential penalizing penetration; such a design may be analysed in terms of energy conservation or dissipation, leading to convenient stability conditions. Implementation issues for the resulting algorithms will be discussed. Various perceptual features will be illustrated, as well as numerical features such as strict energy conservation/disspation, and the degree of interpenetration. Extensions to the "doubly nonlinear" case of geometrically nonlinear string vibration in conjunction with distributed collision will also be discussed.

# 1 Introduction

Many musical instruments feature collision interactions—clearly crucial to any instrument relying on percussive impact (such as, e.g., pianos or percussion instruments), but which also play a role in problems involving distributed collision with a barrier, as in the case of various Indian stringed instruments such as the the sitar [1] and timbura, and further when collision between vibrating components is present, as in the case of the snare drum.

Presented here is a brief investigation of numerical design for such systems, taking the simple test case of the string with a unilateral constraint [2]—such a model necessarily involves a non-smooth (one-sided) nonlinearity. One approach to numerical design for such a problem employs a hard non-penetrative constraints to model the collision—another employs a penalty formulation [3], smoothing the nonlinearity, but allowing for some spurious interpenetration of the vibrating object (the string in this case) into the barrier. As is the case for other nonlinear systems in musical acoustics [4], an approach based on a Hamiltonian formulation is invaluable, allowing for both stability conditions as well as, in this case, bounds on interpenetration. The collision problem has been treated previously by various authors, using both finite difference time domain methods [5] and digital waveguide techniques [6], for sound synthesis. Further recent results on Hamiltonian numerical methods for collisions, for a wide variety of systems in musical acoustics, may be found in [7].

In Section 2, a simple model of a stiff lossy string vibrating in a single transverse polarization against a barrier is presented, accompanied by an energy analysis. Section 3 describes the transfer of such a Hamiltonian model to a discrete formulation; various distinct approximations to the system available in the discrete case, all of which lead, ultimately, to a numerical energy conserving (dissipating) design, from which stability conditions may be deduced. Simulation results appear in Section 4.

# 2 String/barrier Collision Model

Consider a stiff string, vibrating at low amplitude in a single transverse polarization, and in contact with a barrier. For simplicity, only the unforced problem will be treated here. One model of such a string is given by

$$\mathcal{L}[u] - \mathcal{F} = 0 \tag{1}$$

Here $u(x,t)$ is the displacement of the string, as a function of $t \geq 0$, and for $x \in \mathcal{D} = [0, L]$, for a string length $L$. The linear operator $\mathcal{L}$ is defined here as

$$\mathcal{L}[u] = (\rho\partial_{tt} - T\partial_{xx} + EI\partial_{xx}\partial_{xx} + 2\rho\sigma_0\partial_t - 2\rho\sigma_1\partial_t\partial_{xx})\,[u] \tag{2}$$

Here, $\partial_t$ and $\partial_x$ represent partial differentiation with respect to $t$ and $x$. $\rho$ is linear mass density, in kg/m, $T$ is string tension in N, $E$ is Young's modulus, in Pa, $I$ is moment of inertia, in m$^4$. $\sigma_0, \sigma_1 \geq 0$ are parameters allowing for frequency dependent loss. When $\sigma_0 = \sigma_1 = 0$, the string is lossless. In the absence of $\mathcal{F}$, this equation describes the unforced motion of a string under linear conditions. In this basic study, boundary conditions are assumed simply supported, i.e. $u = \partial_{xx}u = 0$ at $x = 0, L$. For this unforced problem, two initial conditions, $u(x,0)$ and $\partial_t u(x,0)$ must be supplied.

The term $\mathcal{F}(x,t)$ is a force density, representing the effect of string collision with a rigid barrier below, located at height $b(x)$. In a numerical implementation, it is convenient to model this barrier as perfectly elastic collision, but allowing for a small amount of interpenetration of the string into the barrier. Consider a force density of the form

$$\mathcal{F} = \mathcal{F}(\eta) \qquad \eta = b - u \tag{3}$$

depending on the penetration distance $\eta(x,t)$—a necessary requirement is that $\mathcal{F} = 0$ whenever and wherever $\eta \leq 0$. Such a force should penalize interpenetration, and, in order to be numerically tractable, should be smooth. One choice is

$$\mathcal{F} = K[\eta]_+^\alpha \qquad [\eta]_+ = \frac{1}{2}(\eta + |\eta|) \tag{4}$$

for some constants $K > 0$, and $\alpha > 1$. Such a power-law form resembles that found in Hertzian models of collision [8], and often used in models of the hammer-string interaction [9]; here however, it is used as an approximation to an ideal collision [10], and is best thought of as a mathematical construction, rather than a physical one. A more useful way of writing the penalty force density corresponding to the power law is in terms of a potential density $\phi(\eta)$, as

$$\mathcal{F} = \partial_t\phi/\partial_t\eta \qquad \phi(\eta) = \frac{K}{\alpha+1}[\eta]_+^{\alpha+1} \geq 0 \tag{5}$$

Through multiplication of (1) by $\partial_t u$, and using integration by parts over $\mathcal{D}$, an energy balance results:

$$\frac{d\mathfrak{H}}{dt} = -\mathfrak{Q} \tag{6}$$

where the total stored energy $\mathfrak{H} = \mathfrak{H}_L + \mathfrak{H}_B$ and dissipated power $\mathfrak{Q}$ are given by

$$\mathfrak{H}_L = \int_{\mathcal{D}} \frac{\rho}{2}(\partial_t u)^2 + \frac{T}{2}(\partial_x u)^2 + \frac{EI}{2}(\partial_{xx}u)^2\, dx \tag{7}$$

$$\mathfrak{H}_B = \int_{\mathcal{D}} \phi\, dx \quad \mathfrak{Q} = \int_{\mathcal{D}} 2\rho\left(\sigma_0(\partial_t u)^2 + \sigma_1(\partial_x u)^2\right) dx \tag{8}$$

In particular, simply supported boundary conditions have been employed here. Note in particular that $\mathfrak{H} \geq 0$ and $\mathfrak{D} \geq 0$ implying that, under unforced conditions, the system is dissipative as a whole, i.e. $0 \leq \mathfrak{H}(t) \leq \mathfrak{H}(0)$. In a numerical setting, determining conditions for dissipativity is a convenient means of proving numerical stability, and in this case, for finding bounds on maximal spurious penetration of the string into the barrier.

One could proceed in the opposite sense and deduce the equations of motion (1) through the Euler-Lagrange equations—in numerical design, where energy conservation and dissipation properties are to be enforced, there is no essential difference between the two formulations, i.e., one arrives ultimately at the same algorithms.

# 3 Numerical Methods: FDTD

Consider an approximation of system (1) using finite difference time domain (FDTD) methods [11]. To this end, define the $(N-1)$ element column vector $\mathbf{u}^n = [u_1^n, \ldots, u_{N-1}^n]^T$, representing an approximation to $u(x,t)$ at time $t = nk$, for some time step $k$, and at interior locations on the string $x_l = lh$, $l = 1, \ldots, N-1$, where $h = L/N$ is the grid spacing, for some integer $N$.

## 3.1 Difference Operators

Time shift operators $e_{t+}$ and $e_{t-}$ may be defined, for any vector $\mathbf{w}^n$, as

$$e_{t+}\mathbf{w}^n = \mathbf{w}^{n+1} \qquad e_{t-}\mathbf{w}^n = \mathbf{w}^{n-1} \tag{9}$$

and, from these basic shifts, forward, backward and centered approximations to a time derivative as

$$\delta_{t+} = \frac{1}{k}(e_{t+}-1) \quad \delta_{t-} = \frac{1}{k}(1-e_{t-}) \quad \delta_{t\cdot} = \frac{1}{2k}(e_{t+}-e_{t-}) \tag{10}$$

and a second time derivative as

$$\delta_{tt} = \delta_{t+}\delta_{t-} = \frac{1}{k^2}(e_{t+} - 2 + e_{t-}) \tag{11}$$

Averaging operators may be defined as

$$\mu_{t+} = \frac{1}{2}(e_{t+} + 1) \quad \mu_{t-} = \frac{1}{2}(1 + e_{t-}) \qquad \mu_{tt} = \mu_{t+}\mu_{t-} \tag{12}$$

Forward and backward spatial differentiation operations $\mathbf{D}_{x+}$ and $\mathbf{D}_{x-}$ may be written, in matrix form, as

$$\mathbf{D}_{x+} = \frac{1}{h}\begin{bmatrix} 1 & & & \\ -1 & 1 & & \\ & \ddots & \ddots & \\ & & -1 & 1 \\ & & & -1 \end{bmatrix} \qquad \mathbf{D}_{x-} = -\mathbf{D}_{x+}^T$$

Here, $\mathbf{D}_{x+}$ is $N \times (N-1)$, and the matrix transpose operation is written here as $^T$. Approximations to the second and fourth spatial derivatives may be written as

$$\mathbf{D}_{xx} = \mathbf{D}_{x-}\mathbf{D}_{x+} \qquad \mathbf{D}_{xxxx} = \mathbf{D}_{xx}\mathbf{D}_{xx} \tag{13}$$

## 3.2 Finite Difference Scheme

A basic finite difference scheme for system (1) may be written, in operator form, as

$$\mathfrak{l}\mathbf{u}^n - \mathfrak{f}^n = 0 \tag{14}$$

Here, the discrete operator $\mathfrak{l}$ is an approximation to the continuous operator $\mathcal{L}$, as defined in (2). Many choices are available—here are two:

$$\mathfrak{l}_\gamma = \rho\left(1 - \frac{\gamma h^2}{4}\mathbf{D}_{xx}\right)\delta_{tt} - T\mathbf{D}_{xx} + EI\mathbf{D}_{xxxx} + 2\rho\delta_{t\cdot}(\sigma_0 - \sigma_1\mathbf{D}_{xx}) \tag{15a}$$

$$\mathfrak{l}_{unc} = \rho\delta_{tt} - T\mu_{tt}\mathbf{D}_{xx} + EI\mu_{tt}\mathbf{D}_{xxxx} + 2\rho\delta_{t\cdot}(\sigma_0 - \sigma_1\mathbf{D}_{xx}) \tag{15b}$$

The first approximation, parameterized by a real number $\gamma$ (constrained, as will be seen) yields a standard centred scheme for the string equation—in particular, when $\gamma = 0$ and $\sigma_1 = 0$, it is explicit. The second, employing averaging operators $\mu_{tt}$ reduces to an application of the so-called trapezoid rule to temporal derivatives, leading to unconditionally stable algorithms but with very poor numerical dispersion and artificial bandlimiting properties. See Section 4.1. Both (and many others) can be analyzed in terms of numerical energy conservation and dissipation.

In analogy with the definition (5) for the collision interaction force, one may define

$$\mathfrak{f}^n = \delta_{t\cdot}\phi^n/\delta_{t\cdot}\eta^n \qquad \eta^n = \mathbf{b} - \mathbf{u}^n \tag{16}$$

$\mathbf{b}$ is the barrier profile sampled at the locations $x = lh$, $l = 1, \ldots, N-1$, and $\mathfrak{f}^n$ is interpreted as the element-by-element division of two vectors. the vector $\phi^n$ is defined as $\phi^n = \phi(\eta^n)$, using a potential function such as that given in (5).

## 3.3 Energy, Stability and Penetration Bounds

In analogy with the continuous system, one may multiply the discrete system (14) by $h(\delta_{t\cdot}\mathbf{u}^n)^T$ to arrive immediately at the energy balance

$$\delta_{t-}\mathfrak{h} = -\mathfrak{q} \qquad \text{where} \qquad \mathfrak{h} = \mathfrak{h}_L + \mathfrak{h}_B \tag{17}$$

where

$$\mathfrak{h}_B^n = h\mathbf{1}^T\mu_{t+}\phi^n \qquad \mathfrak{q}^n = 2\rho h\left(\sigma_0|\delta_{t\cdot}\mathbf{u}^n|^2 + \sigma_1|\delta_{t\cdot}\mathbf{D}_{x+}\mathbf{u}^n|^2\right) \tag{18}$$

where $\mathbf{1}$ indicates a column vector consisting of ones. Note that by construction, $\mathfrak{h}_B \geq 0$ and $\mathfrak{q} \geq 0$.

The form of $\mathfrak{h}_L$, corresponding to stored energy in the string, depends on the choice of the operator $\mathfrak{l}$. For the choices $\mathfrak{l}_\gamma$ and $\mathfrak{l}_{unc}$, as given in (15), $\mathfrak{h}_L$ is given by

$$\begin{aligned}\mathfrak{h}_{L,\gamma} &= \frac{\rho h}{2}|\delta_{t+}\mathbf{u}^n|^2 + \frac{\rho h^3\gamma}{8}|\delta_{t+}\mathbf{D}_{x+}\mathbf{u}^n|^2 \\ &\quad + \frac{Th}{2}\left(\mathbf{D}_{x+}\mathbf{u}^{n+1}\right)^T\mathbf{D}_{x+}\mathbf{u}^n + \frac{EIh}{2}\left(\mathbf{D}_{xx}\mathbf{u}^{n+1}\right)^T\mathbf{D}_{xx}\mathbf{u}^n\end{aligned} \tag{19}$$

$$\mathfrak{h}_{L,unc} = \frac{\rho h}{2}|\delta_{t+}\mathbf{u}^n|^2 + \frac{Th}{2}|\mu_{t+}\mathbf{D}_{x+}\mathbf{u}^n|^2 + \frac{EIh}{2}|\mu_{t+}\mathbf{D}_{xx}\mathbf{u}^n|^2 \tag{20}$$

The scheme will be stable (i.e., dissipative), when $\mathfrak{h}_L \geq 0$. For the choice $\mathfrak{l}_{unc}$, $\mathfrak{h}_{L,unc}$ is non-negative, and the scheme is unconditionally stable. For the choice $\mathfrak{l}_\gamma$, the energy term $\mathfrak{h}_{L,\gamma}$ is non-negative when $\gamma \geq -1$, and when $h \geq h_{min}$, where

$$h_{min}^2 = \frac{Tk}{2\rho(1+\gamma)}\left(k + \sqrt{k^2 + \frac{16EI\rho}{T^2}}\right) \tag{21}$$

For the free parameter $\gamma$, an excellent choice, obtained through matching the number of numerical degrees of freedom of the scheme with that of the system, is

$$\gamma_* = -1 + \frac{Tk^2}{\rho h_*^2} + 4\frac{EIk^2}{\rho h_*^4} \quad , h_*^2 = \frac{2\pi^2 EI}{T\left(\sqrt{1 + 4\frac{EI\rho\pi^2}{T^2k^2}} - 1\right)} \tag{22}$$

When $\mathfrak{h}_L \geq 0$, the algorithm is numerically stable; going further, under these conditions, one may bound the spurious interpenetration $\eta$ under such conditions as $0 \leq \mathfrak{h}_B \leq \mathfrak{h}$, leading immediately to

$$\max(\eta) \leq \left(\frac{2(\alpha+1)\mathfrak{h}}{Kh}\right)^{\frac{1}{\alpha+1}} \tag{23}$$

which can be made as small as desired using an appropriate collision parameter $K$.

### 3.4 Implementation and Iterative Methods

Regardless of the choice of the approximating operator $\mathfrak{l}$, the scheme (14) may be written, in vector matrix form, as

$$\mathbf{A}\mathbf{u}^{n+1} = \mathbf{B}\mathbf{u}^{n} + \mathbf{C}\mathbf{u}^{n-1} + m\frac{\phi^{n+1}-\phi^{n-1}}{\eta^{n+1}-\eta^{n-1}} \tag{24}$$

where one has, for the cases of the parameterized and unconditionally stable schemes:

$$\mathbf{A}_\gamma = \mathbf{L}+\mathbf{M} \qquad \mathbf{B}_\gamma = \mathbf{P}+2\mathbf{L} \qquad \mathbf{C}_\gamma = -\mathbf{L}+\mathbf{M}$$

$$\mathbf{A}_{unc} = \mathbf{I}+\mathbf{M}-\frac{1}{4}\mathbf{P} \quad \mathbf{B}_{unc} = 2\mathbf{I}+\frac{1}{2}\mathbf{P} \quad \mathbf{C}_{unc} = -\mathbf{I}+\frac{1}{4}\mathbf{P}+\mathbf{M}$$

in terms of the matrices

$$\mathbf{L} = \mathbf{I}-\frac{\gamma h^2}{4}\mathbf{D}_{xx} \quad \mathbf{M} = k(\sigma_0-\sigma_1\mathbf{D}_{xx}) \quad \mathbf{P} = \frac{k^2}{\rho}(T\mathbf{D}_{xx}-E\mathbf{I}\mathbf{D}_{xxxx})$$

or, after introducing the variable $\mathbf{r} = \eta^{n+1} - \eta^{n-1}$, as

$$\mathbf{A}\mathbf{r} + \mathbf{g} + m\frac{\phi(\mathbf{r}+\mathbf{a})-\phi(\mathbf{a})}{\mathbf{r}} = 0 \tag{25}$$

where $m = k^2/\rho, \mathbf{g} = \mathbf{B}\mathbf{u}^n + (\mathbf{C}-\mathbf{A})\mathbf{u}^{n-1}$ and $\mathbf{a} = \eta^{n-1}$.

This vector nonlinear equation can be shown to possess a unique solution, when $\mathbf{A}$ is positive definite (as it is here), and for a power law potential of the form given in (5). See, e.g., [7], extending the result for the case of the lumped mass/barrier collision in [12]. An iterative method will be required in general, such as Newton Raphson; the number of iterations required depends strongly on the choice of the parameters defining the barrier power law potential—generally, the larger the value of $K$, the more iterations will be required (and the smaller the spurious interpenetration will be, as per (23)).

If $\mathbf{A}$ is diagonal (i.e., if the scheme is explicit), then the system (25) decouples to a set of scalar nonlinear equations, of the form

$$r_l + \hat{g}_l + \hat{m}\frac{\phi(r_l+a_l)-\phi(a_l)}{r_l} = 0\,,\ l = 1,\ldots,N-1 \tag{26}$$

reducing the computational load. Furthermore, if one makes the choice $\alpha = 1$, corresponding to a quadratic potential, then each scalar equation may be solved exactly, according to the following cases:

$$a_l \geq 0, \hat{g}_l \leq a_l(1-\hat{m}) : r_l = -\frac{\hat{g}_l + 2a_l\hat{m}}{1+\hat{m}}$$

$$a_l \geq 0, \hat{g}_l > a_l(1-\hat{m}) : r_l = -\frac{1}{2}\left(\hat{g}_l + \sqrt{\hat{g}_l^2 + 4\hat{m}a_l^2}\right)$$

$$a_l < 0, \hat{g}_l \geq a_l : r_l = -\hat{g}_l$$

$$a_l < 0, \hat{g}_l < a_l : r_l = \frac{-\hat{g}_l - 2a_l\hat{m} + \sqrt{\hat{g}_l^2 + 4\hat{m}a_l(\hat{g}_l - a_l)}}{2(1+\hat{m})}$$

Such an exact solution leads to a great acceleration with respect to an iterative solver.

## 4 Simulation Results

### 4.1 Approximations to the Linear String: Mode Detuning and Dispersion

Spurious numerical dispersion is a drawback of FDTD approaches to musical instrument simulation and synthesis. For a linear string, for example, in isolation, it leads to a mistuning of modal frequencies. The choice of the linear operator $\mathfrak{l}$ must thus be made carefully. In this section, the dispersive characteristics of three schemes for the string in isolation are examined: using $\mathfrak{l}_\gamma$ with $\gamma = 0$ (the default scheme), the optimal scheme with $\gamma = \gamma_*$, where $\gamma_*$ is as given in (22), and using the unconditional scheme with $\mathfrak{l}_{unc}$.

In Figure 1, the frequency responses of the three schemes are compared, for a typical stiff string—as expected, the optimal scheme gives an excellent match to modal frequencies over a wide range of frequencies—indeed, it is also more efficient than the default scheme. The unconditionally stable scheme exhibits severe warping of modal frequencies in the low audio range. The flipside to such modal accuracy is easily visible in plots of dispersion of a short raised cosine pulse used as an initial condition, as shown in Figure 2, in comparison with a solution computed at a very high sample rate (and thus serving as an approximation to an exact solution)—the unconditionally stable scheme exhibits severe distortion.

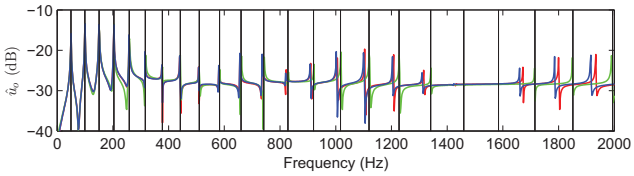


Figure 1: Comparison of frequency responses of different schemes (red: default, green: optimal and blue: unconditionally stable), with exact modal frequencies indicated by plack lines. In this case, the string has parameters: $L = 0.8$ m, $T = 38.5$ N, $r = 0.5$ mm, and is assumed made of steel, with $E = 2\times10^{11}$ Pa and $\rho/\pi r^2 = 7850$ kg/m$^3$. The initial condition is a short raised cosine pulse, and the sample rate is 44 100 Hz.

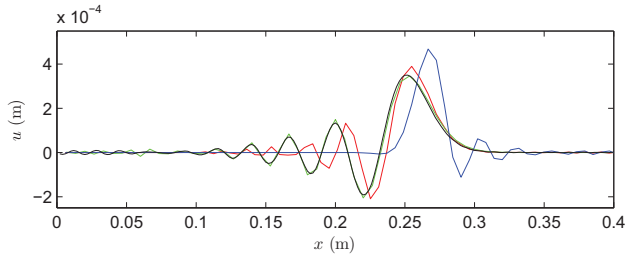


Figure 2: Profile of string, as described in the caption to Figure 1, using different schemes (color coded as above), and using a short raised cosine as an initial condition. The sample rate is 44 100 Hz—in black, a solution computed at 384 kHz (effectively exact) is shown.

### 4.2 Time Evolution of a Plucked String Profile

Continuing the above analysis, now consider the string in contact with a rigid barrier of simple parabolic form, using

the optimal scheme with $\gamma = \gamma_*$. The time evolution of the string profile, illustrating multiple collisions, is as shown in Figure 3.

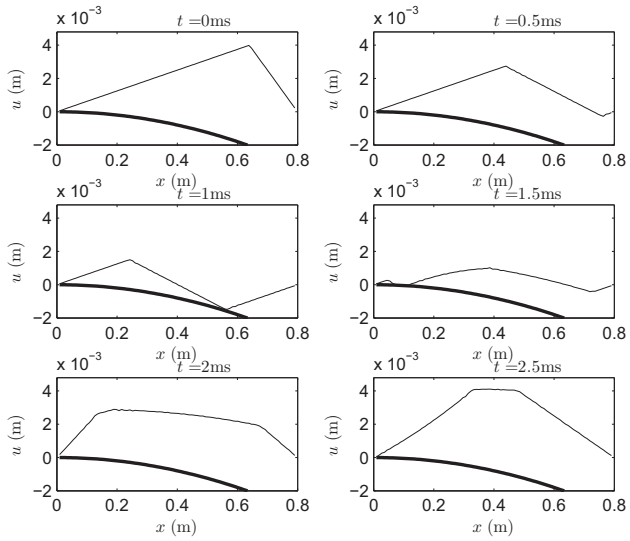


Figure 3: Snapshots of string profile, under a triangular initial distribution, of height 4 mm, in contact with a barrier of parabolic shape, at times as indicated. Sample rate is 44 100 Hz, and string parameters are as in the caption to Figure 1, but with $r = 0.1$ mm. The barrier has parameters $K = 10^{13}$ and $\alpha = 2.3$.

### 4.3 Energy Conservation and Spurious Penetration

Under lossless conditions, the schemes presented here are energy conserving to machine accuracy—see Figure 4, showing the energy partition and energy deviation as a function of time for the string collision as described in the previous section.

For the string/barrier combination described here, the maximum penetration is bounded by (23), giving, in this case, a penetration bound of $1.3{\times}10^{-4}$ m. In fact, as illustrated in the bottom panel of Figure 4, in practice, this bound is overly conservative.

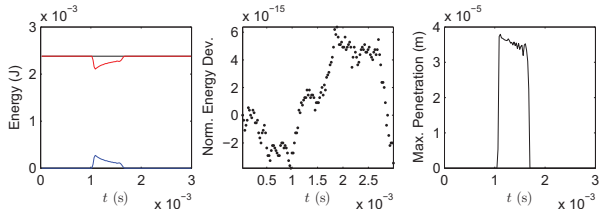


Figure 4: For the simulation described in Figure 3: Left: the energy partition, with string energy in red, and barrier potential energy in blue, and total energy in black. Middle: normalized energy deviation, defined as $\left(\mathfrak{h}^n - \mathfrak{h}^0\right)/\mathfrak{h}_0$. Right: maximum penetration, as a function of time.

### 4.4 Contact Region

The contact region between the string and barrier varies in a highly nontrivial way—indeed, the regions of contact may not be contiguous, as illustrated in Figure 5. In this figure, and interesting phenomenon of sharpening of a wavefront, as well as a "binding" to the barrier during transit is illustrated.

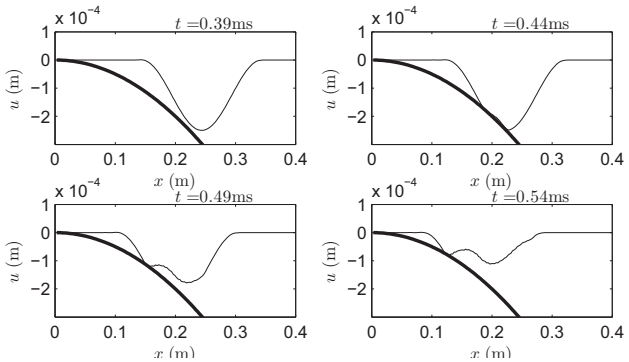


Figure 5: Microfeatures of a leftward-traveling pulse interacting with a smooth barrier, illustrating a non-contiguous contact region, and wave sharpening/binding to the barrier.

### 4.5 Pitch Changes

A more perceptually relevant feature is the effective change in pitch with excitation amplitude, accompanied by the generation of noise-like timbres. Under lossy conditions,

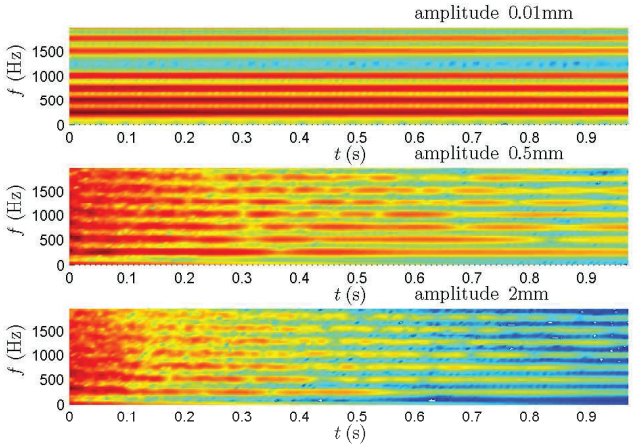


Figure 6: Spectrograms of output, for strings initialized with a triangular distribution, of varying amplitudes, as indicated.

## 5 Conclusion

Hamiltonian based numerical methods provide a number of benefits in the context of collision modeling, as illustrated here in the simple case of a string vibrating under a unilateral constraint. One is the ability to arrive at convenient numerical stability conditions, which result from (a) designing a method such that a given quantity (energy) is either conserved or strictly dissipated, and (b) finding conditions under which this quantity is a non-negative function of the state, thus serving as a Lyapunov function. Another, particularly relevant here, is the ability to extract bounds on spurious interpenetration, so as to have some confidence in the accuracy of computed solutions. As

illustrated here, with the proper choice of penalty potential, such penetration may be made as small as desired. A third benefit is at the level of programming—the energy function may be monitored, at an intermediate stage, as a means of detecting coding errors.

For the continuous problem, the Hamiltonian is uniquely defined, to within a constant. For numerical methods, however, for a given problem, there is an infinite variety of such energy functions, each corresponding to a separate numerical methods (and, though not discussed here, to distinct allowable numerical boundary conditions). Another important point here, then, is one has some freedom to design high-accuracy methods (such as the scheme with $\gamma = \gamma_*$ here)—in particular, analytically attractive methods such as the unconditionally stable scheme do not give good results in comparison.

The bottleneck in such schemes, ultimately, will be the numerical method used to solve a single vector nonlinear equation of the form of (25)—indeed, vector nonlinear equations of such a form occur under in much more general settings involving collisions—see [7]. In general, it would appear that for an iterative method (such as, e.g., Newton Raphson), the number of iterations depends on the degree of allowable interpenetration—one aspect not touched upon here is convergence of Newton's method for such a nonlinear equation (though existence and uniqueness are guaranteed).

# Appendix: Extension to Nonlinear Kirchhoff-Carrier String Model

The numerical method presented here can easily be extended, within the Hamiltonian framework, to include effects of inherent nonlinearity in the string itself. For example, consider the extension:

$$\mathcal{L}[u] + \mathcal{K}[u] - \mathcal{F} = 0 \tag{27}$$

The operator $\mathcal{K}[u]$ is a simple averaged model of nonlinearity in the string, due to Kirchhoff [13] and Carrier [14]:

$$\mathcal{K}[u] = \frac{EA}{2L}\left(\int_{\mathcal{D}} (\partial_x u)^2 \, dx\right) \partial_{xx} u \tag{28}$$

Such a model leads to an effective increase in wave speed (and thus pitch) at high amplitudes, and is sometimes referred to as tension modulation [15]—pitch glide effects are thus captured by such a model. This model also leads to an energy balance of the form given in (6), where now, $\mathfrak{H} = \mathfrak{H}_L + \mathfrak{H}_B + \mathfrak{H}_K$, where

$$\mathfrak{H}_K = \frac{EA}{8L}\left(\int_{\mathcal{D}} \partial_x u \, dx\right)^2 \tag{29}$$

Such an energy balance follows through to an extension of the scheme (14) to

$$\mathfrak{l}[\mathbf{u}^n] + \mathfrak{k}[\mathbf{u}^n] + \mathfrak{f}^n = 0 \tag{30}$$

where

$$\mathfrak{k}[\mathbf{u}^n] = \frac{EA}{2L}\left(\mathbf{D}_{x+}\mathbf{u}^n\right)^T \left(\mu_t \mathbf{D}_{x+}\mathbf{u}^n\right) \mathbf{D}_{xx}\mathbf{u}^n \tag{31}$$

and where now, the energy balance is as given in (17), with $\mathfrak{h} = \mathfrak{h}_L + \mathfrak{h}_B + \mathfrak{h}_K$, where

$$\mathfrak{h}_K = \frac{EAh^2}{8L}\left(\left(\mathbf{D}_{x+}\mathbf{u}^n\right)^T \mathbf{D}_{x+}\mathbf{u}^{n+1}\right)^2 \tag{32}$$

# Acknowledgments

This work was supported by the European Research Council, under grant number StG-2011-279068-NESS.

# References

[1] S. Siddiq. A physical model of the nonlinear sitar string. *Arch. Acoust.*, 37(1):73–79, 2012.

[2] M. Schatzman. A hyperbolic problem of second order with unilateral constraints: The vibrating string with a concave obstacle. *J. Math. Anal. Appl.*, 73:138–191, 1980.

[3] D. Harmon. *Robust, Efficient, and Accurate Contact Algorithms*. PhD thesis, Columbia University, 2010.

[4] S. Bilbao. *Numerical Sound Synthesis*. John Wiley and Sons, Chichester, UK, 2009.

[5] A. Krishnaswamy and J. O. Smith III. Methods for simulating string collisions with rigid spatial obstacles. In *IEEE Workshop on Appl. of Siqnal Processing to Audio and Acoust.*, pages 233–236, New Paltz, New York, October 2003.

[6] D. Kartofelev, A. Stulov, H.-M. Lehtonen, and V. Välimäki. Modeling a vibrating string terminated against a bridge with arbitrary geometry. In *Proc. Stockholm Musical Acoust. Conf.*, Stockholm, Sweden, August 2013.

[7] S. Bilbao, A. Torin, and V. Chatziioannou. Numerical modeling of collisions in musical instruments, 2014. Under review: submitted version available at `http://arxiv.org/abs/1405.2589`.

[8] G. Horvay and A. Veluswami. Hertzian impact of two elastic spheres in the presence of surface damping. *Acta Mechanica*, 35:285–290, 1980.

[9] X. Boutillon. Model for piano hammers: Experimental determination and digital simulation. *J. Acoust. Soc. Am.*, 83(2):746–754, 1988.

[10] R. Fetecau, J. Marsden, M. Ortiz, and M. West. Nonsmooth lagrangian mechanics and variational collision integrators. *SIAM J. Appl. Dyn. Sys.*, 2(3):249–276, 2003.

[11] J. Strikwerda. *Finite Difference Schemes and Partial Differential Equations*. Wadsworth and Brooks, Pacific Grove, California, 1989.

[12] V. Chatziioannou and M. van Walstijn. An energy conserving finite difference scheme for simulation of collisions. In *Proc. Stockholm Musical Acoust. Conf.*, Stockholm, Sweden, 2013.

[13] G. Kirchhoff. *Vorlesungen über Mechanik*. Tauber, Leipzig, 1883.

[14] G. F. Carrier. On the nonlinear vibration problem of the elastic string. *Quarterly of Applied Mathematics*, 3:157–165, 1945.

[15] V. Välimäki, T. Tolonen, and M. Karjalainen. Plucked-string synthesis algorithms with tension modulation nonlinearity. In *Proc. IEEE Int. Conf. Acoust., Speech, Sig. Proc.*, volume 2, pages 977–980, Phoenix, Arizona, March 1999.